A KINETIC APPROACH FOR THE EVALUATION OF DAMPING IN MICRO-ELECTRO-MECHANICAL SYSTEMS DEVICES VIBRATING AT HIGH FREQUENCIES

SILVIA LORENZANI AND LAURENT DESVILLETTES

ABSTRACT. The mechanism leading to gas damping in Micro-Electro-Mechanical Systems (MEMS) devices vibrating at high frequencies is investigated by using the linearized Boltzmann equation based on the ellipsoidal statistical (ES) model. Knowing that walls with different physical structures are used in designing micromachines, general boundary conditions of Maxwell's type have been considered to describe the gas-wall interactions.

keywords: Micro-Electro-Mechanical Systems (MEMS), sound wave resonances, linearized Boltzmann equation.

classification51.10.+y, 45.10.Db, 47.45.Ab

1. INTRODUCTION

Micro-Electro-Mechanical Systems (MEMS) devices have received growing attention in recent years. This is due not only to the excitement naturally associated with a nascent technology, but also because of the great promise of increased miniaturization and performance of MEMS devices over conventional systems. In particular, microstructures vibrating at high frequencies (ranging from 1 MHz to 60 GHz) find applications in inertial sensing, acoustic transduction, optical signal manipulation and RF (radio frequency) components [1, 2, 3, 4, 5]. Such high frequency devices have become a major research area because they should enable a miniaturization and an integration of RF components, with applications to ultra low-power wireless and adaptive/secure telecommunications.

In MEMS devices, the fluid is usually trapped under or around the vibrating micromechanical structure in extremely narrow gaps. As the structure vibrates, it pushes and pulls the fluid film creating complex pressure patterns that depend on the geometry of the structure, the boundary conditions, frequency of oscillations and thickness of the fluid film. In particular, when a planar microstructure oscillates in the direction perpendicular to its surface, the forces exerted by the fluid due to the built-up pressure are always against the movement of the structure. Thus, the fluid-film (typically an air-film) acts as a damper and the phenomenon is called squeeze film damping. Besides the viscous forces that dominate at low frequencies, gas compressibility and inertial forces determine the amount of damping at higher oscillation frequencies. Very recently, gas damping in RF MEMS systems has been studied by using the linearized Navier-Stokes equations with slip boundary conditions for temperature in [6, 7]. Since the analysis presented in [6, 7] failed

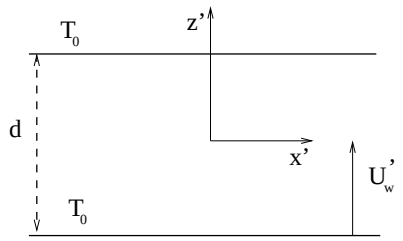

FIGURE 1. Channel geometry.

to predict the correct value of the damping force due to air in a RF MEMS disk resonator [1, 2], in the current paper, we investigate the mechanism leading to gas damping in MEMS devices vibrating at high frequencies within the framework of kinetic theory of rarefied gas.

2. PROBLEM FORMULATION

Let us consider a monatomic gas confined between two flat, infinite, and parallel plates located at $z' = -d/2$ and $z' = d/2$. Both boundaries are held at a constant temperature T_0. The upper wall of the channel (located at $z' = d/2$) is fixed while the lower one (located at $z' = -d/2$) harmonically oscillates in the z'-direction (normal to the wall itself) with angular frequency ω' (the corresponding period being $T' = 2\pi/\omega'$). The basic geometry of the two-dimensional gas layer is outlined in Fig.1 The velocity U'_w of the oscillating plate depends on time t' through the formula

$$U'_w(t') = U'_0 \sin(\omega' t'), \tag{1}$$

where it is assumed that the amplitude U'_0 is very small compared to the thermal velocity v_0, i.e.

$$U'_0 << v_0, \qquad v_0 = \sqrt{2RT_0}, \tag{2}$$

with R being the gas constant and T_0 being the equilibrium temperature of the gas.

Under these conditions, the Boltzmann equation modeling the gas motion inside the channel can be linearized about a Maxwellian f_0 by putting [8, 9]

$$f = f_0(1 + h), \tag{3}$$

where $f(z', \mathbf{c}, t')$ is the distribution function for the molecular velocity $\mathbf{c}$ expressed in units of v_0 and $h(z', \mathbf{c}, t')$ is the small perturbation on the basic equilibrium state. The above mentioned Maxwellian function is given by

$$f_0 = \rho_0 \pi^{-\frac{3}{2}} \exp(-c^2), \tag{4}$$

where ρ_0 is the equilibrium density of the gas. Using Eq. (3), the nonstationary linearized Boltzmann equation reads as

$$\frac{\partial h}{\partial t'} + c_z \frac{\partial h}{\partial z'} = Lh, \tag{5}$$

where Lh is the linearized collision operator. Since it is difficult to manage the Boltzmann operator L as such, for both analytical computations and numerical simulations, simplified kinetic models of the exact collision integral are widely used in practice. Because of its simplicity, the Bhatnagar, Gross and Krook (BGK) model is one of the most popular of these kinetic models [10], although it is known to have a serious flaw: it leads to a wrong Prandtl number (i.e. the dimensionless ratio of viscosity and thermal conductivity). This difficulty can be dealt with when one works in the linearized framework since viscosity and temperature effects are then decoupled [11, 12]. However, for the specific problem with which we are dealing here, where the sound waves generated by the oscillating plate propagate through the gas across the gap of the channel, both temperature variations and thermal conductivity must be accounted for due to compressibility effects. Thus, in order to correctly describe both mass and heat transfer, it is worth investigating the problem with a more refined model than the BGK. We shall therefore use the ellipsoidal statistical (ES) model, which allows one to recover the right Prandtl number [13, 14]. The linearized ES model gives rise to the following collision operator

$$Lh = \tilde{\theta}^{-1}\Big[\rho + 2\mathbf{c}\cdot\mathbf{v} + \tau\,(\mathbf{c}^2 - 3/2) - \lambda\, c_i\, c_j\, P_{ij} + \lambda\,(\rho+\tau)\,\mathbf{c}^2/2 - h\Big], \tag{6}$$

where $\tilde{\theta}$ is a suitable mean free time, while the dimensionless macroscopic perturbed density ρ, velocity $\mathbf{v}$, temperature τ and stress tensor P_{ij} are obtained by taking the moments of h

$$\rho = \pi^{-3/2} \int_{-\infty}^{+\infty} h\, e^{-\mathbf{c}^2}\, d\mathbf{c}, \tag{7}$$

$$\mathbf{v} = \pi^{-3/2} \int_{-\infty}^{+\infty} \mathbf{c}\, h\, e^{-\mathbf{c}^2}\, d\mathbf{c}, \tag{8}$$

$$\tau = \pi^{-3/2} \int_{-\infty}^{+\infty} (\frac{2}{3}\mathbf{c}^2 - 1)\, h\, e^{-\mathbf{c}^2}\, d\mathbf{c}, \tag{9}$$

$$P_{ij} = \pi^{-3/2} \int_{-\infty}^{+\infty} c_i\, c_j\, h\, e^{-\mathbf{c}^2}\, d\mathbf{c}. \tag{10}$$

In Eq. (6), λ is a constant to be chosen in such a way that the correct Prandtl number is obtained, that is

$$P_r = c_p \frac{\mu}{k}, \tag{11}$$

where c_p is the specific heat at constant pressure, μ the viscosity and k the thermal conductivity. λ is equal to 0 for the BGK model ($P_r = 1$) and 1 for a Maxwell gas ($P_r = 2/3$). For a general monoatomic gas the relation between λ and P_r is given by

$$P_r = \frac{2}{2+\lambda}, \tag{12}$$

i.e.,

$$\lambda = \frac{2}{P_r} - 2. \tag{13}$$

In order to get the same viscosity coefficient from the BGK model and the present one, we must put

$$\tilde{\theta} = \frac{(\lambda+2)}{2}\theta, \tag{14}$$

where $\theta = \mu/P_0$ is the collision time defined in the BGK model (with P_0 being the equilibrium pressure). It is convenient now to rescale all variables appearing in Eqs. (5) and (6) as follows

$$t = \frac{t'}{\theta}, \qquad x = \frac{x'}{v_0\theta}, \qquad z = \frac{z'}{v_0\theta}, \tag{15}$$

so that the dimensionless ES linearized equation reads

$$\frac{\partial h}{\partial t} + c_z \frac{\partial h}{\partial z} = \frac{2}{(2+\lambda)} \Big[\rho + 2\mathbf{c}\cdot\mathbf{v} + (\mathbf{c}^2 - 3/2)\,\tau - \lambda\, c_i\, c_j\, P_{ij} + \lambda\, \mathbf{c}^2(\rho+\tau)/2 - h \Big]. \tag{16}$$

Appropriate boundary conditions must be supplied for the Boltzmann equation (16) to be solved. Assuming the diffuse-specular reflection condition of Maxwell's type and specializing the analysis to symmetric gas-wall interactions (so that an accommodation coefficient α can be defined), the boundary conditions (under the assumption (2)) read as [15, 16, 17]

$$\begin{aligned} h(z=-\delta/2,\mathbf{c},t) &= \alpha(\sqrt{\pi}+2\,c_z)\,U_w + (1-\alpha)\,4\,c_z\,U_w \\ &\quad +(1-\alpha)\,h(z=-\delta/2,c_x,c_y,-c_z,t) \\ -\frac{2\,\alpha}{\pi}\int_{-\infty}^{\infty}\int_{-\infty}^{\infty} d\tilde{c}_x d\tilde{c}_y \int_{\tilde{c}_z<0} d\tilde{c}_z \tilde{c}_z\, e^{-\tilde{\mathbf{c}}^2}\, h(z=-\delta/2,\tilde{\mathbf{c}},t) &\qquad c_z>0, \end{aligned} \tag{17}$$

$$h(z=\delta/2,\mathbf{c},t) = (1-\alpha)\,h(z=\delta/2,c_x,c_y,-c_z,t) \tag{18}$$

$$+\frac{2\,\alpha}{\pi}\int_{-\infty}^{\infty}\int_{-\infty}^{\infty} d\tilde{c}_x d\tilde{c}_y \int_{\tilde{c}_z>0} d\tilde{c}_z \tilde{c}_z\, e^{-\tilde{\mathbf{c}}^2}\, h(z=\delta/2,\tilde{\mathbf{c}},t)$$

where $\delta = d/(v_0\theta)$ is the rarefaction parameter (inverse Knudsen number). In Eq. (17), U_w is the dimensionless wall velocity given by

$$U_w(t) = U_0\,\sin(\omega\,t), \tag{19}$$

with $U_w = U_w'/v_0$, $U_0 = U_0'/v_0$, $\omega = \theta\,\omega'$, $T = 2\pi/\omega = T'/\theta$.

Since the problem under consideration is one-dimensional in space, the unknown perturbed distribution function h, as well as the overall quantities, depend only on the z coordinate. Likewise, we can reduce the dimensionality of the molecular-velocity space by introducing the following projection procedure [18, 19]. First, we multiply Eq. (16) by $\frac{1}{\pi}\,e^{-(\mathbf{c_x}^2+\mathbf{c_y}^2)}$ and we integrate over all c_x and c_y. Then, we multiply Eq. (16) for a second time by $\frac{1}{\pi}\,({c_x}^2+{c_y}^2-1)\,e^{-(\mathbf{c_x}^2+\mathbf{c_y}^2)}$ and we integrate again over all c_x and c_y. The resulting equations after the projection are

$$\frac{\partial H}{\partial t} + c_z\,\frac{\partial H}{\partial z} + \frac{2}{(2+\lambda)}\,H \tag{20}$$

$$= \frac{2}{(2+\lambda)}\left[\rho + 2\,c_z\,v_z + (c_z^2-1/2)\,\tau - \lambda\,(c_z^2-1/2)\,P_{zz} + \frac{\lambda}{2}\,(c_z^2-1/2)(\rho+\tau)\right],$$

and

$$\frac{\partial \Psi}{\partial t} + c_z\,\frac{\partial \Psi}{\partial z} + \frac{2}{(2+\lambda)}\,\Psi = \frac{2}{(2+\lambda)}\left[\tau - \frac{\lambda}{4}(\rho+\tau) + \frac{\lambda}{2}P_{zz}\right], \tag{21}$$

where the reduced unknown distribution functions H and Ψ are defined as

$$H(z,c_z,t) = \frac{1}{\pi}\int_{-\infty}^{+\infty}\int_{-\infty}^{+\infty} h(z,\mathbf{c},t)\,e^{-(c_x^2+c_y^2)}\,dc_x\,dc_y, \tag{22}$$

and

$$\Psi(z,c_z,t) = \frac{1}{\pi}\int_{-\infty}^{+\infty}\int_{-\infty}^{+\infty} (c_x^2+c_y^2-1)\,h(z,\mathbf{c},t)\,e^{-(c_x^2+c_y^2)}\,dc_x\,dc_y, \tag{23}$$

respectively. In order to derive Eqs. (20) and (21) in their final form, we have considered the linearized equation of state

$$P = \frac{1}{3}\left[P_{xx}+P_{yy}+P_{zz}\right] = \frac{1}{2}\,(\rho+\tau), \tag{24}$$

with P being the dimensionless perturbed pressure of the gas. The macroscopic fields appearing on the right-hand side of Eqs. (20) and (21) are defined by

$$\rho(z,t) = \frac{1}{\sqrt{\pi}} \int_{-\infty}^{+\infty} H\, e^{-c_z^2}\, dc_z, \tag{25}$$

$$v_z(z,t) = \frac{1}{\sqrt{\pi}} \int_{-\infty}^{+\infty} c_z\, H\, e^{-c_z^2}\, dc_z, \tag{26}$$

$$\tau(z,t) = \frac{1}{\sqrt{\pi}} \int_{-\infty}^{+\infty} \frac{2}{3} \left[(c_z^2 - 1/2)\, H + \Psi \right] e^{-c_z^2}\, dc_z, \tag{27}$$

$$P_{zz}(z,t) = \frac{1}{\sqrt{\pi}} \int_{-\infty}^{+\infty} c_z^2\, H\, e^{-c_z^2}\, dc_z. \tag{28}$$

The elimination of one (or more) component of the molecular velocity by a projection procedure is quite important for the computational efficiency of the numerical scheme. The reduced distribution functions H and Ψ must satisfy the following boundary conditions coming from Eqs. (17) and (18)

$$H(z=-\delta/2, c_z, t) = \alpha\, (\sqrt{\pi} + 2\, c_z)\, U_w + (1-\alpha)\, 4\, c_z\, U_w \tag{29}$$

$$+(1-\alpha)\, H(z=-\delta/2, -c_z, t) - 2\,\alpha \int_{\tilde{c}_z<0} d\tilde{c}_z\, \tilde{c}_z\, e^{-\tilde{c}_z^2}\, H(z=-\delta/2, \tilde{c}_z, t) \;\; ; c_z > 0,$$

$$\Psi(z=-\delta/2, c_z, t) = (1-\alpha)\, \Psi(z=-\delta/2, -c_z, t) \tag{30}$$

$$H(z=\delta/2, c_z, t) = (1-\alpha)\, H(z=\delta/2, -c_z, t) + \tag{31}$$

$$2\,\alpha \int_{\tilde{c}_z>0} d\tilde{c}_z\, \tilde{c}_z\, e^{-\tilde{c}_z^2}\, H(z=\delta/2, \tilde{c}_z, t) \qquad\qquad c_z < 0,$$

$$\Psi(z=\delta/2, c_z, t) = (1-\alpha)\, \Psi(z=\delta/2, -c_z, t) \tag{32}$$

The time-dependent problem described by Eqs. (20) and (21), with boundary conditions given by Eqs. (29)-(32), has been numerically solved by a deterministic finite-difference method presented in detail in [20, 21]. In order to compute the damping force exerted by the gas on the moving wall of the channel, the perturbation of the normal stress P_{zz} (defined by Eq. (28)) has to be evaluated at $z = -\delta/2$. Therefore, our numerical code has been validated in [22] by comparing the values of the amplitude and of the phase of P_{zz} at the oscillating wall determined by means of a numerical integration of Eqs. (20) and (21), with the highly accurate results obtained in [19] from a numerical solution of the linearized Shakhov kinetic equation, in the case of complete diffuse reemission ($\alpha = 1$) at the channel walls. The normal stress time-dependence is of the following known form:

$$|P_{zz}|\,\sin(\omega\,t+\phi), \tag{33}$$

where $|P_{zz}|$ is the amplitude and ϕ the phase. In general, the amplitude of the time-dependent macroscopic fields is extracted from our numerical results as half the vertical distance between a maximum and the nearest minimum appearing in the temporal evolution of the macroscopic quantity. This corresponds to the definition

$$|A(z,t)| = [\mathcal{R}e(A)^2 + \mathcal{I}m(A)^2]^{1/2}, \tag{34}$$

where $\mathcal{R}e$ and $\mathcal{I}m$ denote the real and imaginary part, respectively, of the field $A(z,t)$. Instead, the phase can be recovered from our simulations through the application of a chi-square fit to the functional form of the expression (33) [23, 24]. The good agreement shown by the comparison between our findings and the results obtained in [19], by using the Shakhov model, reveals not only the reliability of our numerical method of solution, but also the weak dependence of the normal stress field (evaluated at the moving channel wall) on the collisional model used.

3. RESULTS AND DISCUSSION

Low frequency MEMS devices are normally operated at very low pressure in order to minimize the damping due to the internal friction of the gas flowing in the small gaps between the moving parts of these microstructures (viscous damping). This need can be overcome when MEMS devices vibrate at relatively high frequencies, since gas compressibility and inertial forces lead then to another damping mechanism related to the occurrence of sound wave resonances which take place in the direction normal to the channel walls. Corresponding to a resonant response of the system, the amplitude of P_{zz} at $z=-\delta/2$ reaches its maximum value (resonance) or its minimum value (antiresonance). The occurrence of an antiresonance is particularly important since if the device is operated close to the corresponding frequency, the damping due to the gas (measured by the amplitude of $P_{zz}(z=-\delta/2,t)$) is considerably reduced. In the case of complete diffuse reemission ($\alpha=1$), we found a scaling law (valid for all Knudsen numbers) that predicts a resonant response of the system when the dimensionless distance between the channel walls (measured in units of the oscillation period of the moving plate)

$$L=\frac{\delta}{T}=\frac{d\,\omega'}{2\,\pi\,v_0} \tag{35}$$

takes a well-defined fixed value. Note that the quantity $(2\,\pi\,v_0/\omega')$ is the distance traveled by gaseous molecules during one cycle of oscillation of the moving boundary. In [22], the values of L corresponding to the main resonances have been analytically derived for $\alpha=1$:

$$L_a \simeq 0.21 \quad (\text{antiresonance})$$

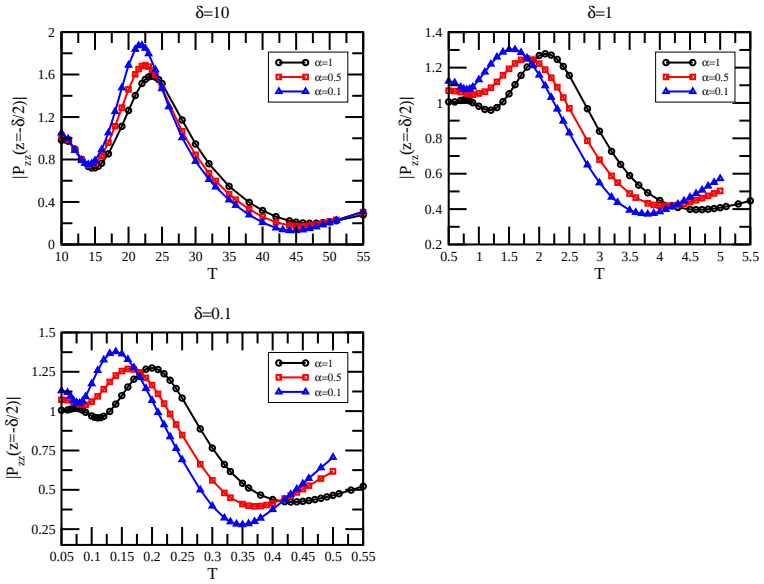

FIGURE 2. Amplitude of the normal stress tensor P_{zz} at the oscillating wall versus T for different values of the rarefaction parameter δ. In each panel, the three plots correspond to the following values of the accommodation coefficient α: $\alpha = 1$ (circles), $\alpha = 0.5$ (squares), $\alpha = 0.1$ (triangles).

$$L_r \simeq 0.48 \quad (\text{resonance}).$$

Once these approximated fixed values, L_a and L_r, have been determined, Eq. (35) allows one to compute the values of T for the occurrence of resonances and antiresonances for different values of the rarefaction parameter δ progressing from free molecular, through transitional, to continuum regions (since the ratio $L = \delta/T$ must assume always the same constant value each time the system undergoes a resonant response).

It is worth noting that the double degenerate geometry considered here, that is, infinitely long and wide channels, does not affect in any way the results obtained, since the numerical simulations carried out in [22] have shown that, above a certain frequency of oscillation, the sound wave propagation takes place only in the z-direction across the gap. This fully trapped gas situation greatly simplifies the analysis since the topology of the damper becomes insignificant and the problem can be reduced to a 1-dimensional one.

A change in the boundary conditions, obtained by assuming $\alpha \neq 1$, breaks the scaling law as expressed by Eq. (35). This is clearly shown in Fig. 2, where the profiles of the normal stress amplitude at the oscillating wall are plotted as a function of the period T, for three different values of the rarefaction parameter δ and of the accommodation coefficient α. While the location of the main resonance (resp. antiresonance) which corresponds to the highest maximum (resp. lowest

minimum) remains almost unchanged in the near-continuum flow limit ($\delta = 10$) by varying α, the influence of the accommodation coefficient becomes evident in the transitional region ($\delta = 1$) and in the near free-molecular flow limit ($\delta = 0.1$). As α decreases, the location of the resonances (antiresonances) moves towards smaller values of T for $\delta = 1$ and $\delta = 0.1$. This means that, for each given $\alpha \neq 1$, the dimensionless distance between the channel walls, L, defined by Eq. (35), does not assume a fixed constant value any longer.

Furthermore, even if the value of $|P_{zz}(z = -\delta/2)|$ corresponding to the main resonant and antiresonant frequencies is a nonmonotonic function of α, at a fixed δ, the value taken by the normal stress amplitude at the oscillating wall, in correspondence of an antiresonant response of the system, reaches its minimum in the limit $\alpha \to 0$.

Then, at a fixed α, the value of $|P_{zz}(z = -\delta/2)|$ corresponding to the main antiresonant frequency decreases by increasing δ. Therefore, squeezed-film dampers vibrating at high frequencies, unlike the low frequency MEMS devices, do not need to operate at very low pressure in order to minimize the damping due to gas flow, greatly reducing the need for (and cost associated with) vacuum packaging. This effect has been already noticed in the experimental testing of micromechanical resonators vibrating at high frequencies [1, 5] and in a preliminary numerical investigation [6, 7] but, up to now, it has not received a complete theoretical justification.

4. ACKNOWLEDGMENTS

The authors are grateful to the franco-italian project GREFI-MEFI for its financial support. S. Lorenzani also thanks 'Fondazione Cariplo' for the support of her research activity.

REFERENCES

[1] J. R. Clark, W.-T. Hsu, C. T.-C. Nguyen, *Technical Digest IEEE Int. Electron Devices Meeting*, 493-496 (2000).
[2] B. Bircumshaw, G. Liu, H. Takeuchi, T.-J. King, R. Howe, O. O'Reilly, A. Pisano, *Proceedings of Transducers'03* (Boston, MA), 875-878 (2003).
[3] Z. Hao, S. Pourkamali, F. Ayazi, *J. Microelectromechanical Systems* **13**, 1043-1053 (2004).
[4] S. Pourkamali, Z. Hao, F. Ayazi, *J. Microelectromechanical Systems* **13**, 1054-1062 (2004).
[5] J. R. Clark, W.-T. Hsu, M. A. Abdelmoneum, C. T.-C. Nguyen, *J. Microelectromechanical Systems* **14**, 1298-1310 (2005).
[6] T. Veijola and A. Lehtovuori, *Symposium on Design, Test, Integration and Packaging of MEMS/MOEMS*. DTIP 2007, Stresa, Italy, pp. 156-161 (2007).
[7] T. Veijola and A. Lehtovuori, *J. Sound Vib.* **319**, 606-621 (2009).
[8] C. Cercignani, *The Boltzmann Equation and Its Applications*, Springer, New York (1988).
[9] Y. Sone, *Molecular Gas Dynamics: Theory, Techniques, and Applications*, Birkhäuser, Boston (2007).
[10] P. L. Bhatnagar, E. P. Gross, M. Krook, *Phys. Rev.* **94**, 511-525 (1954).
[11] F. Sharipov and V. Seleznev, *J. Phys. Chem. Ref. Data* **27**, 657-706 (1998).
[12] L. B. Barichello, M. Camargo, P. Rodrigues, C. E. Siewert, *Z. angew. Math. Phys.* **52**, 517-534 (2001).
[13] C. Cercignani and G. Tironi, *Il Nuovo Cimento* **43**, 64-78 (1966).

[14] C. Cercignani, M. Lampis, S. Lorenzani, *Transp. Theory Stat. Phys.* **36**, 257-280 (2007).
[15] S. K. Loyalka and T. C. Cheng, *Phys. Fluids* **22**, 830-836 (1979).
[16] M. M. R. Williams, *Z. angew. Math. Phys.* **52**, 500-516 (2001).
[17] R. D. M. Garcia and C. E. Siewert, *Z. angew. Math. Phys.* **57**, 94-122 (2006).
[18] S. Naris and D. Valougeorgis, *Phys. Fluids* **17**, 097106-097106-12 (2005).
[19] D. Kalempa and F. Sharipov, *Phys. Fluids* **21**, 103601-103601-14 (2009).
[20] S. Lorenzani, L. Gibelli, A. Frezzotti, A. Frangi, C. Cercignani, *Nanoscale Microscale Thermophys. Eng.* **11**, 211-226 (2007).
[21] A. Frangi, A. Frezzotti, S. Lorenzani, *Computers & Structures* **85**, 810-817 (2007).
[22] L. Desvillettes and S. Lorenzani, , submitted (2012).
[23] N. G. Hadjiconstantinou and A. L. Garcia, *Phys. Fluids* **13**, 1040-1046 (2001).
[24] N. G. Hadjiconstantinou, *Phys. Fluids* **14**, 802-809 (2002).

(S.L.) DIPARTIMENTO DI MATEMATICA, POLITECNICO DI MILANO, MILANO, ITALY 20133

(L.D.) ENS CACHAN, CMLA, CNRS, PRES UNIVERSUD & IUF, CACHAN, FRANCE 94235